

Photometry of the long period dwarf nova MU Centauri¹

Albert Bruch

Laboratório Nacional de Astrofísica, Rua Estados Unidos, 154, CEP 37504-364, Itajubá -
MG, Brazil

(Text published in: New Astronomy, Vol. 46, p. 60 – 72 (2016))

Abstract

Even among the brighter cataclysmic variables an appreciable number of objects exist about which not much is known. One of them, MU Cen, was observed as part of a small project to better characterize these neglected systems. The temporal variations of the brightness of MU Cen during quiescence were studied in order to find clues to the structure of the system and its behaviour on time scales of hours and shorter. Light curves observed in white light at a time resolution of a few seconds and with a duration of several hours, obtained in six nights and spanning a total time base of five months, were investigated using different time series analysis tools, as well as model fits. The light curve of MU Cen is dominated by ellipsoidal variations of the secondary star. The refined orbital period is $P_{\text{orb}} = 0.341883$ days. Model fits permit to constrain the temperature of the secondary star to ~ 5000 K and the orbital inclination to $50^\circ \leq i \leq 65^\circ$. The latter result permits estimates of the component masses which are probably somewhat smaller than derived in previous publications. A second persistent period of $P_2 = 0.178692$ days was also identified. Its origin remains unclear. As all cataclysmic variables, MU Cen exhibits flickering, however, on a rather low level. Its frequency behaviour is normal for quiescent dwarf novae. There are indications that the individual flickering events are not always independent but can lead to effects reminiscent of quasi-periodic oscillations.

Keywords: Stars: binaries: close – Stars: dwarf novae – Stars: individual: MU Cen

1 Introduction

Cataclysmic variables (CVs) are interactive binaries where a late type, low mass star which is normally on or close to the main sequence transfers matter to a white dwarf. Unless strong magnetic fields are present the transferred matter first forms an accretion disk before it settles onto the surface of the compact object. All CVs are expected to suffer from major

¹Based on observations taken at the Observatório do Pico dos Dias / LNA

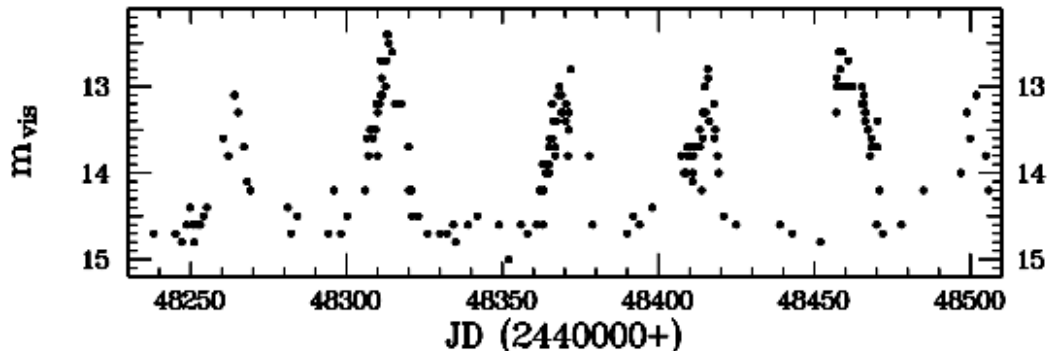


Figure 1: Long term light curve of MU Cen as observed by AAVSO members during the 1991 observing season.

outbursts on secular time scales when they appear as novae. Depending on the detailed conditions, many of them also undergo intermittent less violent outbursts on time scale of weeks, months or years. These are the dwarf novae.

The number of known systems of this kind has grown enormously in recent years. Much of this growth is due to many CVs detected in large scale surveys either as a by-product of their main purpose (e.g., the Sloan Digital Sky Survey) or as results of dedicated searches for transient sources (e.g. Catalina Real-time Transient Survey; MASTER Global Robotic Net). Most of these newly detected CVs are rather faint in their normal brightness state which, in the case of dwarf novae, is the quiescent phase between outbursts. Therefore, the characterization of their individual properties is expensive because it requires large telescopes.

On the other hand, it is much easier to perform detailed studies of the brighter CVs, most of which are known for a long time. It may therefore be expected that these systems are all quite well known. However, this is not the case. Surprisingly, even after decades of intense observations of CVs there is still an appreciable number of known or suspected systems, bright enough (say, $m_{\text{vis}} \leq 15^{\text{m}}$) to be easily observed with comparatively small telescopes, which have not been studied sufficiently to even be certain – in some cases – of their very class membership. I therefore started a small observing program aimed at a better understanding of these so far neglected stars. Here, I report on the results concerning the dwarf nova MU Cen.

In this case there is no doubt about the class membership. MU Cen is well established as a dwarf nova. Fig. 1 shows a section of the long-term AAVSO light curve which encompasses the entire 1991 observing season. The typical alternations between quiescent states at a level of $\sim 14.6^{\text{m}}$ and outbursts reaching $\sim 12.4^{\text{m}}$ leave no doubts about the classification. Colours in the *UBV* system measured by Mumford (1971) and Vogt (1983) are comparatively red for a cataclysmic variable (see Bruch & Engel, 1994), indicating a significant contribution of the cool secondary star and thus a long orbital period.

Descriptions of the spectral characteristics of MU Cen are somewhat ambiguous. Vogt (1976) describes the spectrum at minimum stage as a continuum without strong emission features. Citing a private communication from M.W. Feast, Warner (1976) describes it to be weak, containing narrow hydrogen and possibly He II lines in emission, again during minimum. Vogt's description contrast somewhat with the optical spectrum reproduced in Fig. 14 of Zwitter & Munari (1996) which is fairly normal for a quiescent dwarf nova and is in agreement with Warner's characterization, except that it does not show any trace of

He II.

On the basis of a relation between the colours and orbital periods of quiescent dwarf novae and novae, Vogt (1981) first estimated the period of MU Cen to be 8.8 hours. Later, Friend et al. (1990), using radial velocity measurements of absorption features of the secondary star observed in near infrared spectra in three successive nights, derived a value of $P_{\text{spec}} = 0.342 \pm 0.001$ days (8.208 ± 0.024 hours)².

Time resolved photometric observations of MU Cen are scarce. In particular, no light curve with a time resolution sufficient to show flickering has ever been published. It is well known that accretion of mass via a disk onto a central object normally leads to apparently stochastic brightness variations termed flickering. In CVs they cause variability on timescales typically of the order of minutes and with amplitudes which can range from a few millimagnitudes to more than an entire magnitude. For a general characterization of flickering in CVs, see Bruch (1992). The only photometric measurements of MU Cen consisting of more than isolated brightness measurements have been performed by Echevarría (1988) at a time resolution of ~ 4 -5 minutes during the rise to an outburst on 1986, March 8. Disregarding the long term brightness increase over the ~ 3 hours of observations, the scatter of the data points in the V band remain within $\sim 0.^m05$. In view of the coarse time resolution and the small amplitude it is not clear if this scatter is due to flickering. Therefore, the present observations of MU Cen were initiated with the objective to verify the presence of flickering in this system. But, as will be seen, they revealed much more details about MU Cen than just rapid and erratic brightness variations.

2 Observations

All observations were carried out at the 0.6-m Zeiss and the 0.6-m Boller & Chivens telescopes of the Observatório do Pico dos Dias, operated by the Laboratório Nacional de Astrofísica, Brazil. In order to maximize the count rates in the short exposure intervals necessary to resolve the expected rapid flickering variations no filters were used.

Time series imaging of the field around MU Cen was performed using cameras of type Andor iKon-L936-BV equipped with back illuminated, visually optimized CCDs. Basic data reduction (biasing, flat-fielding) was performed using IRAF. For the construction of light curves aperture photometry routines implemented in the MIRA software system (Bruch, 1993) were employed. The same system was used for all further data reductions and calculations. No attempt was made to calibrate the white light measurements. Brightness was rather measured as magnitude difference of the target star with respect to several comparison stars in the field. A summary of the observations is given in Table 1.

3 The light curve

3.1 General properties

I observed light curves of MU Cen in six nights in 2015 (see Table 1) at a time resolution of $5^s - 6^s$. UCAC4 228-062720 (taken from the Forth USNO CCD Astrograph Catalogue; Zacharias et al., 2013) was used as the primary comparison star. MU Cen did not show large night-to-night variations. Since four of the observing nights are contiguous this shows that the system was not in outburst. A rough estimate, involving the magnitude of UCAC4

²I denote the spectroscopic period of Friend et al. (1990) by P_{spec} in order to distinguish it from the refined orbital period P_{orb} defined later.

Table 1: Journal of observations

Obs. Date	Start (UT)	End (UT)	Time Res. (s)	Number of Integr.
2015 Feb 11	6:00	7:58	5	1 394
2015 May 21/33	21:35	3:15	6	2 728
2015 Jun 08/09	21:59	2:17	5	2 989
2015 Jun 09/10	21:26	1:42	5	2 679
2015 Jun 10/11	21:17	1:13	5	2 761
2015 Jun 11/12	21:18	1:38	5	2 988

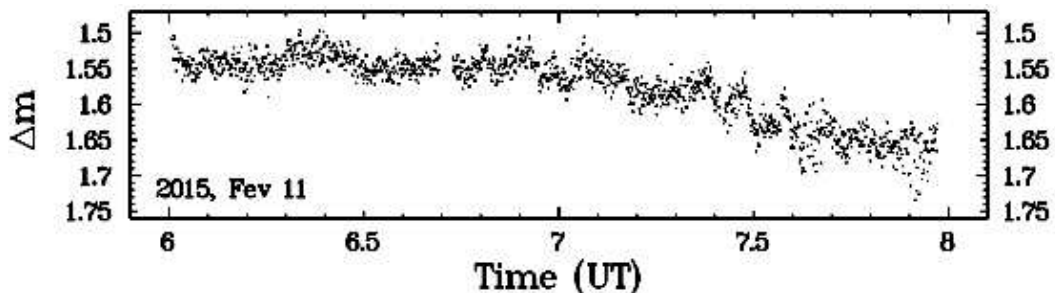


Figure 2: Light curve of MU Cen during the night of 2015, Feb. 11.

228-062720 quoted by Zacharias et al. (2013) ($V = 13^m.031$ and $B = 14^m.022$; meaning that its spectral type is roughly K0), the isophotal wavelength of the observations (~ 5960 Å; right between the V and R bands; see Sect. 5), the expected $V - R$ colour of the dominating MU Cen secondary star (Sect. 5), and the magnitude difference between MU Cen and UCAC4 228-062720, leads to a visual magnitude of MU Cen which is similar to the average quiescent visual magnitude (see Fig. 1).

The (shorter) light curve of 2015, Feb. 11 is shown in Fig. 2. Fig. 3 contains the other light curves. All of them show a clear modulation on a time scale of about 4 hours, i.e., roughly half the spectroscopic period. This suggest immediately ellipsoidal variations of the secondary star which should contribute a significant part of the light in this long period dwarf nova. A more detailed analysis of the variations confirms this suspicion (see below). Superposed on the modulation on hourly time scales are erratic low amplitude short term fluctuations which are compatible with flickering on a rather low scale.

3.2 Periods in the light curve

In order to characterize the variations on time scales of several hours the light curves were combined into a single data set after applying the barycentric correction. In order to take into account possible night-to-night variations of the average brightness, I first performed a sine-fit to the original light curves³ and subtracted the vertical offset of the best fit sine curve.

In order to verify if the brightness modulations are indeed coherent over several nights,

³For the nights of February 11 and June 9 it was necessary to fix the period to $P = 0.5 \times P_{\text{spec}}$ to get consistent results; during the other nights the sine-fit converged to a period very close to $0.5 \times P_{\text{spec}}$.

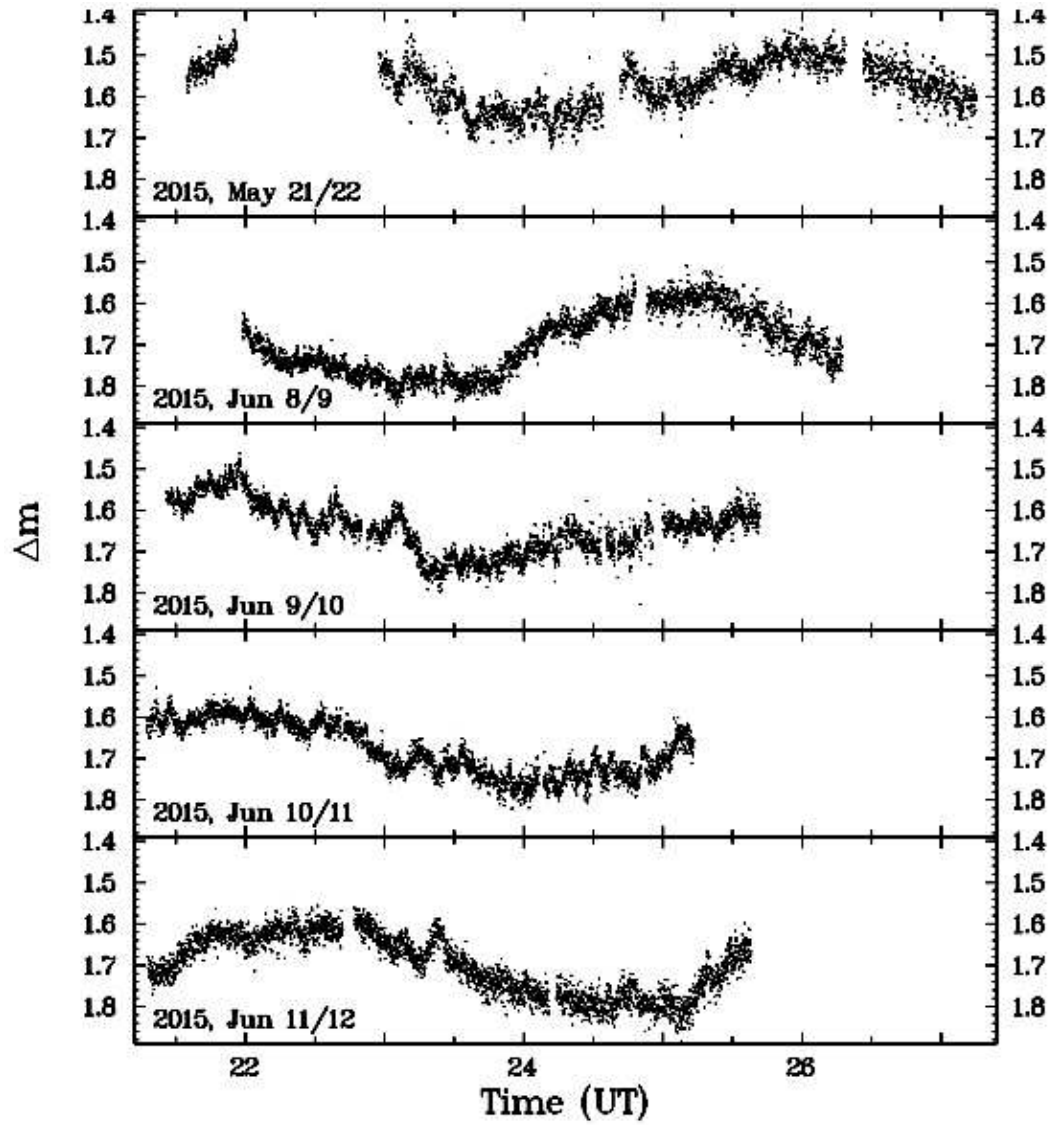


Figure 3: Light curves of MU Cen during several nights in 2015 May and June, plotted on the same time and magnitude scale.

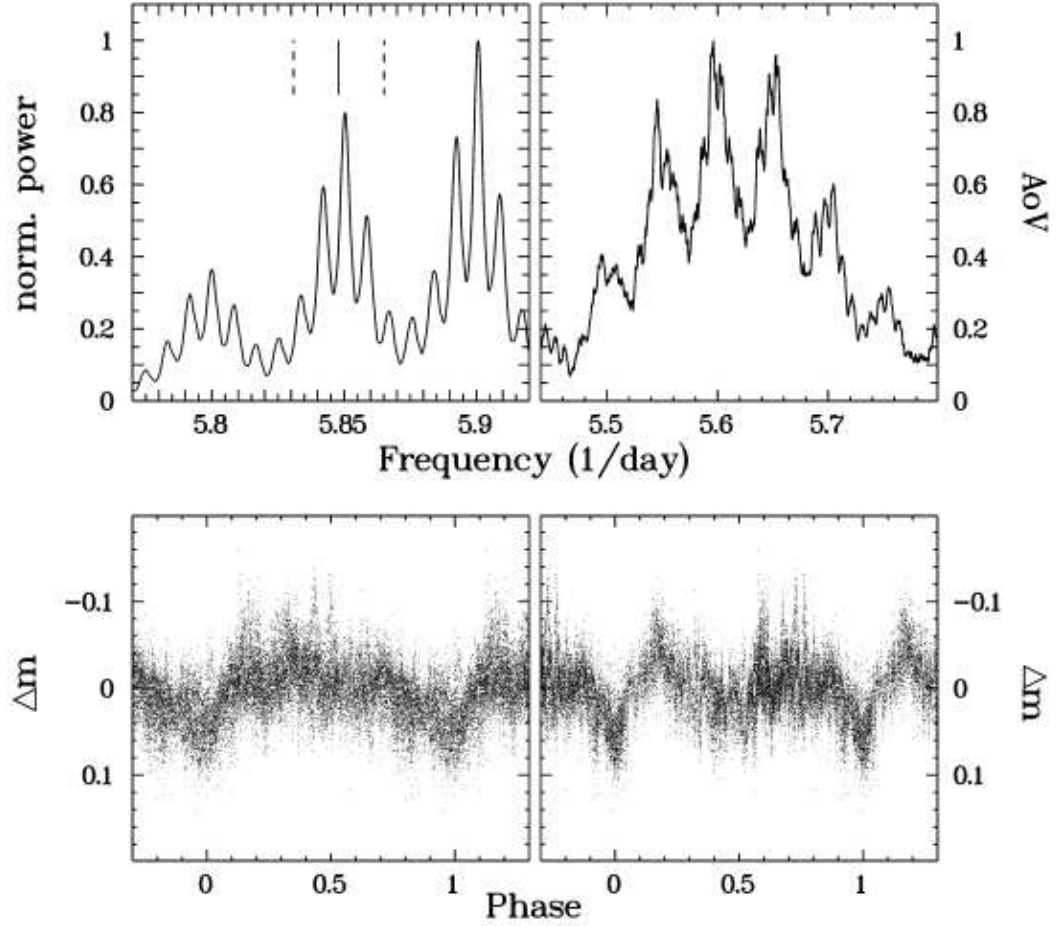


Figure 4: *Upper left frame:* AoV periodogram of the combined light curves of MU Cen, restricted to a narrow frequency range close to 2 times the orbital frequency. The vertical lines mark the frequency and the error limits corresponding to half the spectroscopic period. *Upper right frame:* AoV periodogram of the residuals between the original light curve and a best sine fit with a period fixed to the inverse of the frequency of the orbital peak in the AoV periodogram of the upper left frame. *Lower left frame:* Residual light curve folded on the period P_2 (corresponding to the highest peak in the AoV periodogram of the upper right frame). *Lower right frame:* Residual light curve folded on period $2 \times P_2$.

I first calculated a power spectrum of the combined light curves of the four contiguous observing nights in June, using the Lomb-Scargle algorithm (Lomb 1976, Scargle 1982, Horne & Baliunas 1986). It shows a strong peak at a frequency very close to $2/P_{\text{spec}}$ together with a nice pattern of daily aliases, leaving no doubt about the periodicity of the variations. Next, the combined light curves of all data was subjected to a periodogram analysis. This time, the analysis-of-variance (AoV) algorithm (Schwarzenberg-Czerny, 1989) was preferred which leads to a higher contrast in the periodogram than the Lomb-Scargle power spectrum. An expanded section of the frequency range around $2/P_{\text{spec}}$ is shown in the upper left frame of Fig. 4. It is most interesting that the peak corresponding to $2/P_{\text{spec}}$ [indicated together with the error range quoted by Friend et al. (1990) by the vertical tick marks] is only the second highest peak in the periodogram. Does this mean that the spectroscopic period is slightly in error? After all, it was determined from observations spanning a short time base of only ~ 52 hours or 6.4 cycles. As it will be shown below, this is not the case.

First, however, a sine curve with the period fixed to the period corresponding to the peak close to $2/P_{\text{spec}}$ in the AoV periodogram was fit to the light curve. A second AoV periodogram was then calculated from the residuals between the original data and the best fit sine curve. In the upper right frame of Fig. 4 a restricted frequency interval of this periodogram is shown. It contains several alias peaks. The highest of them corresponds to a period $P_2 = 0.178692$ days which is slightly longer than $0.5 \times P_{\text{spec}}$. The minimum of this modulation can be expressed by the ephemeris:

$$\text{BJD}_{\text{min}} = 2457182.495 (18) + 0.178692 (26) \times E$$

where E is the cycle number. In view of the difficulty to define sound statistical error limits for periods based on power spectra (or AoV periodograms) with complicated window functions and in the presence of flickering (Schwarzenberg-Czerny 1991) only a conservative order of magnitude error (in brackets, expressed in units of the last significant digits of the period) is given, such that it would lead to an easily recognizable phase shift of 0.1 over the total time base of the observations. Similarly, the error of the epoch is simply assumed to be equal to 10% of the period.

The folded light curve is shown in the lower left frame of Fig. 4. The minimum has been chosen as phase 0. Flickering makes the light curve noisy, but there is no doubt about the presence of consistent variations. The wave form is not sinusoidal, but rather exhibits a broad and structured asymmetrical maximum and a narrower minimum.

In order to remove the strong scatter which is due to flickering, the curve folded on P_2 was binned into intervals of 0.01 in phase and subsequently smoothed by a cubic spline fit. This modulation was then subtracted from the combined 2015 light curve which finally was again subjected to a period analysis. The corresponding AoV periodogram is shown in the left frame of Fig. 5. As in Fig. 4 twice the frequency of the spectroscopic variations and their error limits are shown as vertical tick marks. Now the highest peak is very close to $0.5 \times P_{\text{spec}}$.

The much longer time base of the photometric observations, as compared to the radial velocity curve of Friend et al. (1990), permits a refinement of the orbital ephemeris for MU Cen. Interpreting the variations as being due to ellipsoidal variations of the secondary, the minima in the light curve should coincide with the upper and lower conjunction between the cool star and the white dwarf. The right frame of Fig. 5 shows the light curves folded on the refined period $P_{\text{orb}} = 0.341883$ days ($8^{\text{h}}12^{\text{m}}3$) deduced from the AoV periodogram. Light curve minima occur at:

$$\text{BJD}_{\text{min}} = 2457182.459 (34) + 0.341883 (97) \times E$$

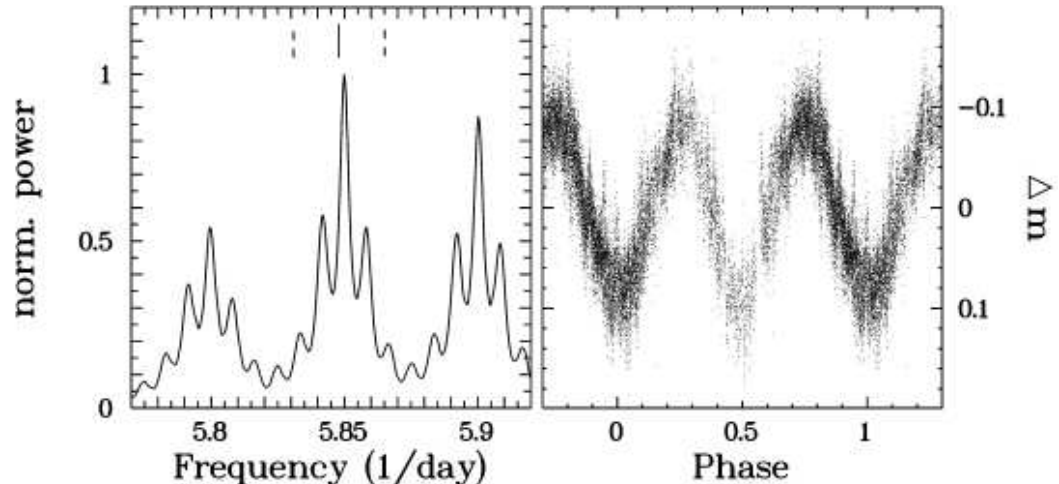


Figure 5: *Left frame:* AoV periodogram of the combined 2015 light curve of MU Cen after subtraction of the modulations with period P_2 (see text). The vertical lines mark the frequency and the error limits corresponding to half the spectroscopic period. *Right frame:* Light curve after subtraction of the modulations with period P_2 , folded on the refined orbital period, i.e., twice the period corresponding to the highest peak of the AoV periodogram in the left frame.

Order of magnitude errors were determined in the same way as for P_2 .

Although the minima have quite similar depth and thus do not permit an immediate decision whether these ephemeris refer to the upper or lower conjunction of the components of MU Cen it will be shown in Sect. 4 that the primary star is in front at phase 0.

The original light curve was investigated for further significant periodic modulations. However, apart from P_{orb} and P_2 , none were found.

3.3 Aperiodic variations: Flickering

It is well known that flickering is a hallmark of cataclysmic variables. It is therefore not surprising that MU Cen also exhibits this phenomenon (see Figs. 2 and 3), albeit with a relatively low amplitude when compared to many other dwarf novae in quiescence. An estimate of its amplitude can be derived from the difference between the folded orbital light curve (right frame of Fig. 5) and its smoothed version (Fig. 9) which will be used in Sect. 4 to adjust a model to the observed data. A range of ± 3 of the standard deviation of this difference may be regarded as the typical flickering amplitude: $A_f = 0^{\text{m}}.16$. This is significantly lower than normally observed in quiescent dwarf novae. From the compilation of Beckemper (1995) an average amplitude of $A_f = 0^{\text{m}}.32 \pm 0^{\text{m}}.17$ can be derived⁴ used a somewhat different method to estimate the flickering amplitude than applied here. However, this does not invalidate the conclusion..

⁴Beckemper (1995)

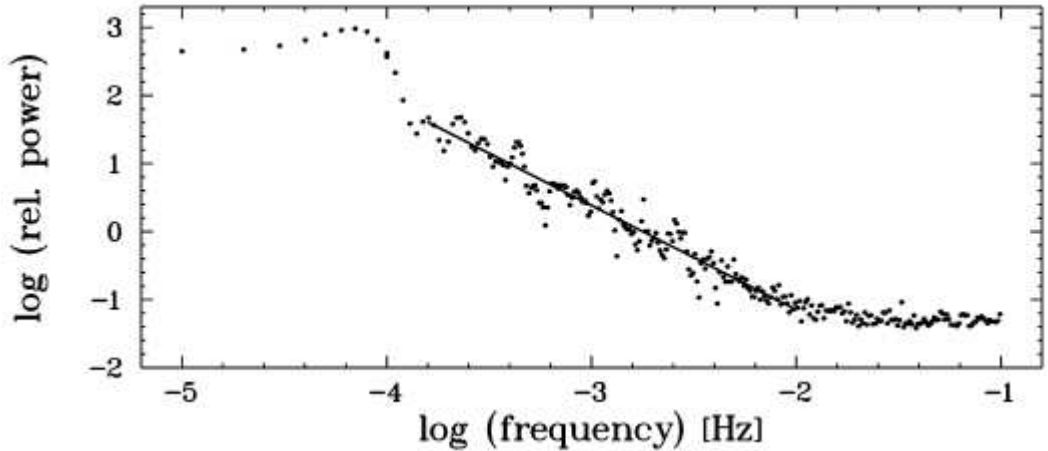


Figure 6: Averaged power spectrum of the light curves of MU Cen (dots). The straight line is a least squares fit to the linear part of the drop of power towards higher frequencies.

3.3.1 Power spectra

In order to establish the quantitative properties of the flickering in MU Cen, I first investigate its frequency spectrum. As is well known, the power spectrum of a light curve is a function of the frequency ν which is proportional to the energy released by variations at that frequency. The energy, in turn, is proportional to the square of the amplitude of the underlying variation. Therefore, the root of the power spectrum can be regarded as a measure of the amplitude of the variations in the light curve at frequency ν [?].

On a double logarithmic scale the power spectra of all light curves of MU Cen, calculated with the Lomb-Scargle algorithm, are remarkably similar. Therefore, their average, binned in phase at intervals of $\Delta \log(\nu) = 0.01$ (frequency expressed in Hertz) was calculated. The result is shown in Fig. 6. As is typically observed in CVs, the power spectrum levels off at low frequencies. The hump close to $\log(\nu) = -4.1$ can be explained by the orbital variations discussed in Sect. 3.2. At higher frequencies the (logarithmic) power P starts to drop linearly with an inclination α , indicating that the flickering behaves like red noise ($P \sim \nu^\alpha$). At still higher frequencies ($\log(\nu) \geq -2$) the power spectrum again levels off, signaling the dominance of random measurement errors, manifest as white noise.

The slope of the linear drop determines the distribution of the relative power of the flickering at different frequencies. It was measured by a least squares fit of a straight line to the data in the interval $-3.83 \leq \log(\nu) \leq -2$ (solid line in Fig. 6). The resulting value $\alpha = -1.532 \pm 0.002$ is close to the upper end of the distribution of corresponding values measured in other CV light curves by Bruch (1992)⁵ and Nollen (1995) which span the range of $-2.64 \leq \alpha \leq -1.24$ ⁶. The comparatively small value of $|\alpha|$ in MU Cen indicates that the dominance of large over small amplitude variations in this system is less strong than in the majority of CVs.

⁵Since Bruch (1992) measured α in the amplitude spectra, his values must be multiplied by two to be compared to the present data.

⁶disregarding the anomalous CV AE Aqr.

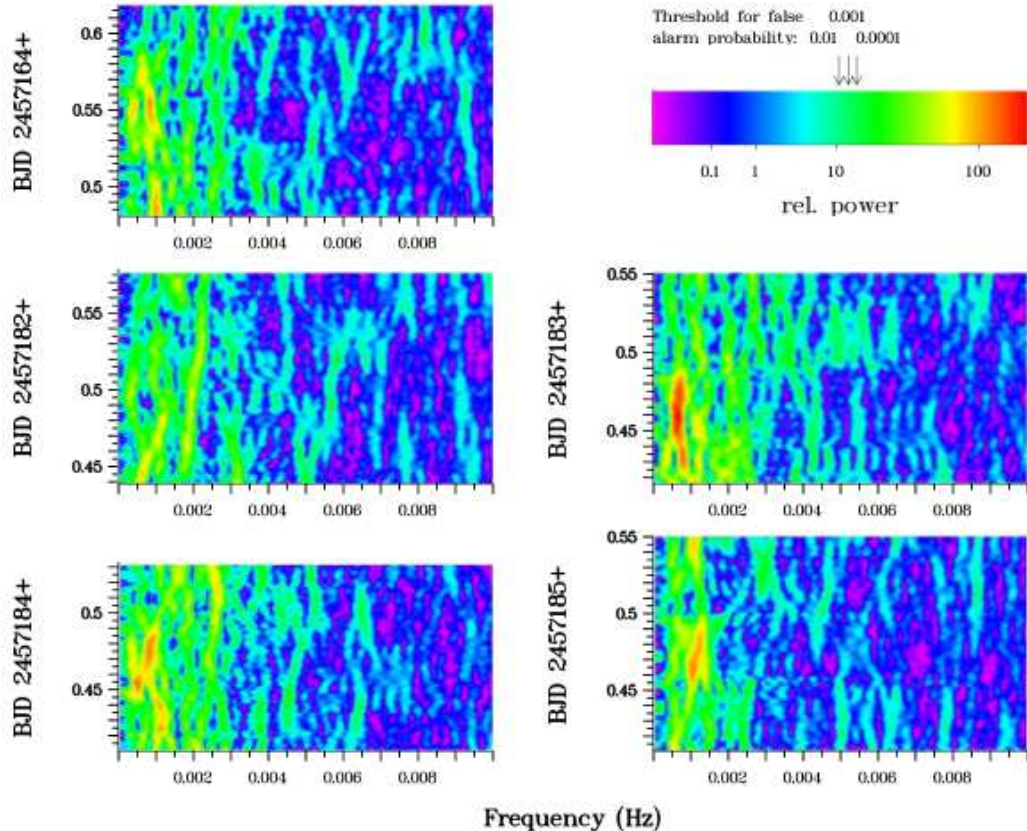


Figure 7: Stacked power spectra of five light curves of MU Cen. Power is shown on a logarithmic scale as a function of frequency and time. Note that structures in vertical direction with an extend of less than ~ 1 hour (about one quarter of the vertical scale) are not independent. The threshold values for false alarm probabilities 0.01, 0.001 and 0.0001 are marked on the colour bar (top right).

3.3.2 Oscillations

In order to verify if the individual events contributing to the flickering are really independent, or if oscillations persistent in time are present, stacked power spectra of the light curves of 2015, May and June⁷ (discarding the data points before the gap in the observations on May 21; Fig. 3) were calculated following Bruch (2014), and are displayed in Fig. 7. Here, the power is shown on a logarithmic scale as a function of frequency (horizontal axis) and time (vertical axis). Note that spectra within a time scale of 1 hour (that is approximately a quarter of the total range in time in all frames) are not independent. Therefore, only structures with a vertical extend of more than an hour indicate persistent signals.

The power levels corresponding to false alarm probabilities (i.e., the probability for a feature in the power spectra to be caused by noise) of 0.01, 0.001 and 0.0001 are indicated on the colour bar in the top right panel of Fig. 7. They were calculated using eq. 18 of Scargle (1982) and depend strongly on the number N_i of independent frequencies in the

⁷The light curve of 2015, Feb. 11, is too short for this exercise.

power spectrum. Horne & Baliunas (1986) have shown that N_i is not only a function of the number of data points from which the power spectrum is calculated, but also depends significantly on the details of data sampling. Following Horne & Baliunas (1986), N_i was here estimated for each light curve by generating 10 000 data sets consisting of pure Gaussian noise, sampled in exactly the same way as the real data. The distribution function of the highest peaks in their power spectra⁸ was constructed and fit to the theoretical distribution curve (eq. 14 of Scargle, 1982) which contains N_i as the only free parameter. Not surprisingly, in view of the similarity of data sampling, N_i is almost the same in the five nights considered here. Therefore, the threshold values for the false alarm probability are practically the same for all power spectra show in Fig. 7.

Some intriguing features can be seen in the stacked power spectra. Maxima which slowly evolve in strength and frequency can extend over the entire duration of a light curve, suggesting the presence of persistent, albeit not coherent oscillations. A particular clear-cut example is present on 2015, Jun 8 (second left hand frame in Fig. 7). During the entire length of the light curve, the power spectra exhibit a maximum which migrates slowly from ~ 0.0016 Hz to ~ 0.0023 Hz (or $\sim 10^m$ to $\sim 7^m$). Similar features appear to be present also during other nights. Other strong signals have a temporal extend of not significantly more than an hour and may therefore be due to individual flickering flares.

The persistent power spectra features seen in some light curves of MU Cen share the characteristics attributed to quasi-periodic oscillations (QPOs) sometimes seen in CVs. They occur on time scales of a couple of minutes, are not stable in frequency and are transient. Warner (2004) gives an overview of the rich phenomenology of such oscillations. The relationship between QPOs and flickering is not clear. Bruch (2014) pointed out that an accidental superposition of random flickering flares, or a physical connection between individual flares may well lead to their interpretation as QPOs. This made him raise the question whether there is a conceptual difference between the two phenomena at all.

3.3.3 Wavelet analysis

The wavelet transform (see Jawerth & Sweldens, 1994, Chui, 1992, and Scargle et al., 1993, for general introductions) is an alternative to the Fourier transform (and thus power spectra) when analyzing stochastic data such as flickering. It permits the decomposition of a signal according to a localized function, the (finite) carrier of which is tied to the investigated scale. The base functions – the wavelets – are scaled versions of a fundamental function, the mother wavelet. The wavelet transform of a time-dependent signal is then a representation of the signal in time and frequency.

The application of wavelet techniques to flickering light curves was pioneered by Fritz & Bruch (1998). They showed that the scalegram [?], which basically measures the variance of the wavelet coefficients and thus of the modulated part of the signal (e.g., a lightcurve) as a function of the time scale, permits, when suitable normalized, a direct comparison between light curves observed under different conditions. They also found that the scalegrams of flickering light curves on a double logarithmic scale always exhibit a linear rise from small to long time scales, when disregarding very small (data noise) or very long (variations not representing flickering) time scales. This enables to condense the essence of the scalegram into two parameters, the slope $\overline{\alpha}^9$ of a straight line fitted to the scalegram points, and

⁸The power spectra were oversampled in order to make sure that individual maxima are resolved and thus an observed peak is in fact close to the maximum of the peak, and not just a point on the rising or falling branch.

⁹Here, the symbol $\overline{\alpha}$ is used in order to avoid confusion with α introduced earlier as the inclination of the linear part of the flickering power spectrum on a double logarithmic scale.

$\Sigma = \log S(t_{\text{ref}})$, where S is the scalegram value and t_{ref} is a reference timescale (for details, see Fritz & Bruch, 1998). $\bar{\alpha}$ measures the distribution of the strength of the flickering among different timescales, while Σ measures the overall strength of the flickering with respect to the unmodulated background light.

The normalized scalegrams of the 2015 May and June light curves of MU Cen are shown in Fig. 8. They are remarkably similar to each other. Even the one deviating graph, corresponding to the light curve of June 9, differs only slightly from the others when compared to the much larger scatter found in different light curves of the same object by Fritz & Bruch (1998). Consequently, the parameters $\bar{\alpha}$ and Σ [choosing 3 minutes as reference time scale as has been done by Fritz & Bruch (1998)] are exceptionally well defined: $\bar{\alpha} = 1.70 \pm 0.10$ and $\Sigma = -1.76 \pm 0.24$. This confines MU Cen to a small range of the $\bar{\alpha} - \Sigma$ diagram at the lower edge of the region occupied by quiescent dwarf novae (see Figs. 12 – 14 of Fritz & Bruch, 1998).

The small (for a quiescent dwarf nova) value of Σ reflects the comparatively low amplitude scale of the flickering in MU Cen. $\bar{\alpha}$, measuring the distribution of the strength of the flickering on different time scales, should not be independent of the inclination α of the linear part of the double logarithmic power spectrum. This is confirmed by the inset in Fig. 8, where $\bar{\alpha}$ is plotted as a function of α for all white light and B -band light curves studied by both, Fritz & Bruch (1998) and Nohlen (1995). In spite of considerable scatter both entities are clearly correlated. The location of MU Cen is indicated by a cross.

4 Model fits

In order to delimit some system parameters of MU Cen, I will compare the observed light curve with results of some simplified model calculations. To this end, I employ the Wilson-Devinney code (Wilson & Devinney, 1971, Wilson, 1979), as implemented in MIRA, in the mode appropriate for semi-detached binaries. It is not the aim of this exercise to model the MU Cen system in detail, but rather to see if the ellipsoidal variations can be reproduced with reasonable system parameters. Therefore, the inadequacy of the Wilson-Devinney code to describe the primary component of a CV (white dwarf, accretion disk, hot spot) does not invalidate the results. As will be seen, a good fit to the data can be achieved with the primary modeled as a moderately hot constant star, influencing the shape of the observed variations only through reflection off the secondary star. Of course, this is not a physical description of the primary, but just a parameterization.

The Wilson-Devinney model involves many parameters. Of these, the following were adjusted to the data: the mass ratio $q = M_2/M_1$ of the components, the orbital inclination i , and, for the secondary star, the temperature T_2 , the limb darkening coefficient u_2 , the gravity darkening coefficient g_2 and the albedo \mathcal{A}_2 . The mass ratio also determines the potential at the Roche surface and thus the radius of the secondary star in units of the component separation. The primary component was parameterized by its temperature and its surface potential (determining its size in the Roche geometry). Moreover, a phase shift was taken into account in order to make up for a possible error in the ephemeris. Finally, the normalization constant was also adjusted.

The isophotal wavelength λ_{iso} of the observed bandpass has only a small influence on the results and was therefore fixed. In order to estimate λ_{iso} , I assume the telescope and atmospheric transmission functions to be constant over the range of sensitivity of the detector. A rough stellar energy distribution function can be obtained assuming the ratio of the radiated energy of the secondary star and the primary component (only considering the contribution of the accretion disk) to be equal to 2.75 in the observed bandpass (see

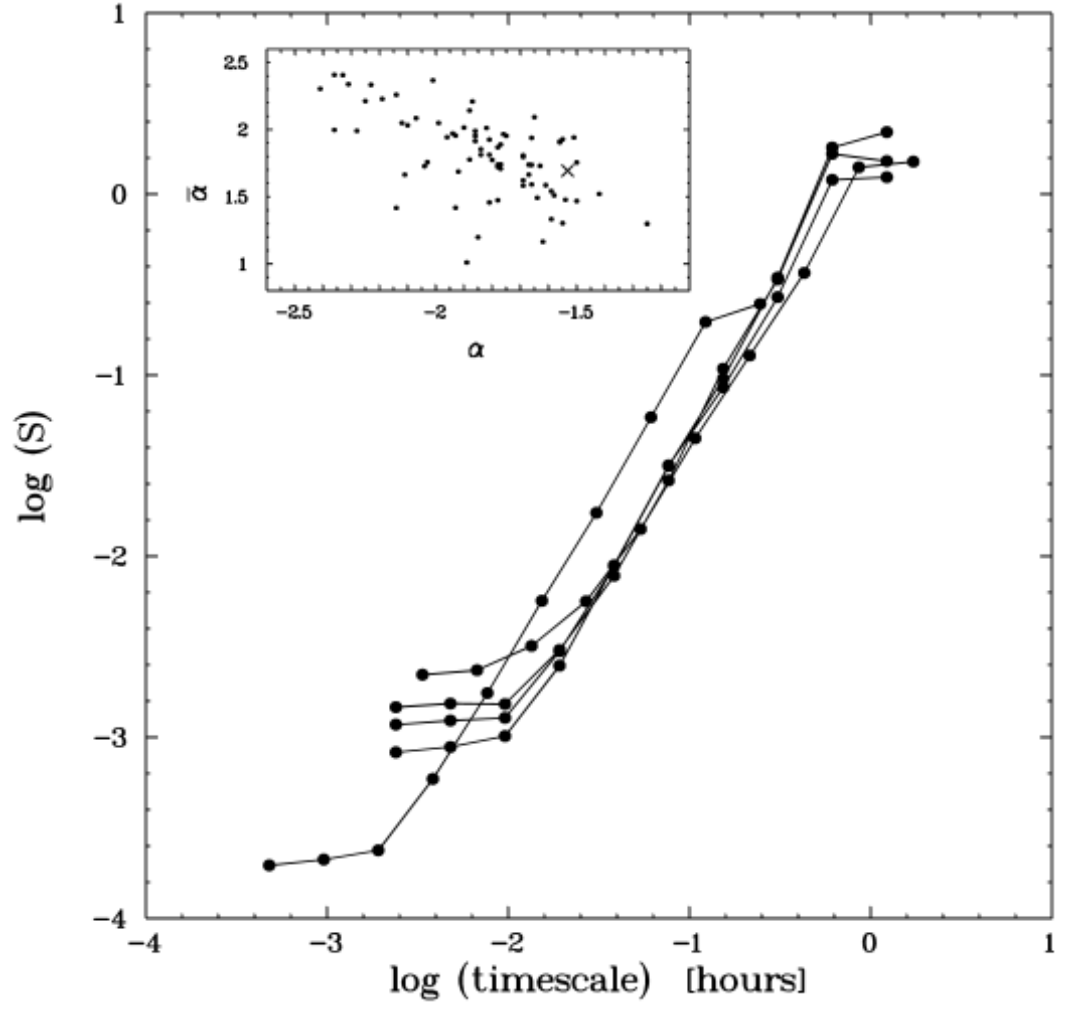


Figure 8: Energy normalized scalegrams of the 1995 May and June light curves of MU Cen. The insert shows the relation between the inclination α of the linear part of the double logarithmic power spectra of flickering light curves (from Nohlen, 1995) and the scalegram parameter $\bar{\alpha}$ (from Fritz & Bruch, 1998). The location of MU Cen is indicated by a cross.

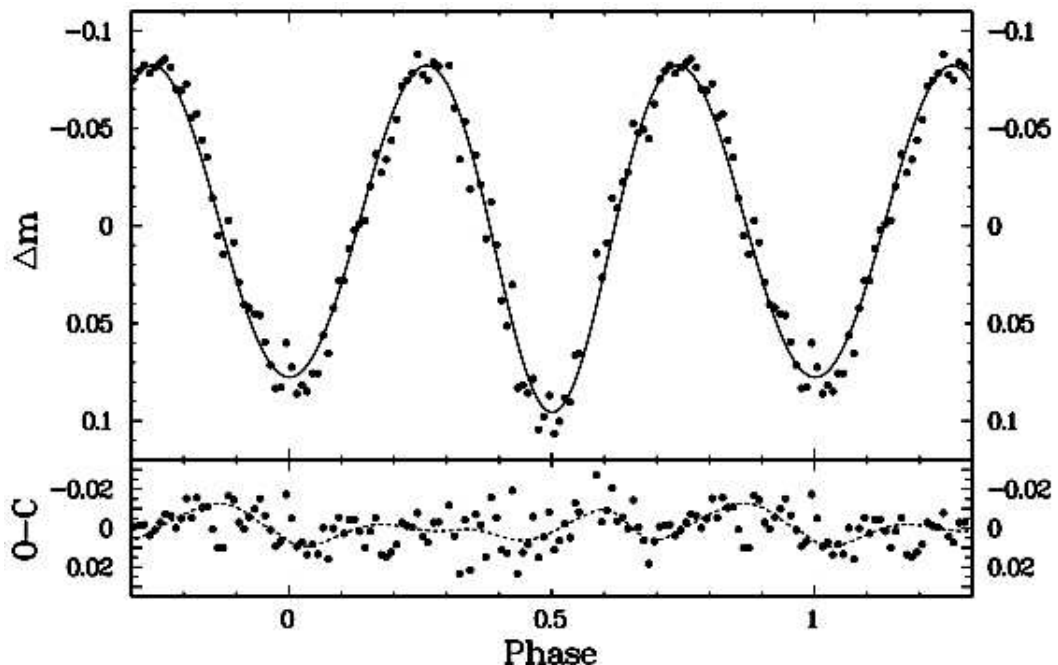


Figure 9: *Upper frame:* Phase folded and binned light curve of MU Cen (dots) and best fit model light curve (solid line). *Lower frame:* Difference between observed and model light curve.

below). The cool star is assumed to radiate like a black body with a temperature of 5 000 K (see below). For the primary a standard steady state accretion disk spectrum is assumed¹⁰, calculated for a mass transfer rate of $10^{-9} M_{\odot}/\text{year}$, a primary star mass of $M_1 = 0.8 M_{\odot}$, an inner disk radius corresponding to the radius of a white dwarf with that mass, and an outer disk radius of $0.4 A$, where A is the component separation calculated from P_{orb} , M_1 and $q = 0.83$ (Friend et al., 1990), using Kepler's law. This approximation to the spectral energy distribution of MU Cen, together with the sensitivity function of the CCD detector used for the observations, then yields an isophotal wavelength of $\sim 5960 \text{ \AA}$.

In order to fit the model to the data, the phase folded light curve of MU Cen was binned into 100 phase bins. Three of them were rejected because they were strongly contaminated by flickering flares which were not sufficiently averaged out after phase folding. The resulting average light curve is shown as dots in the upper frame of Fig. 9.

In contrast to Fig. 5, it now is obvious that the minimum at phase 0.5 is slightly deeper than that at phase 0. This is expected if phase 0 corresponds to the upper conjunction of the secondary star because then the observer sees more of the side illuminated by the primary than during lower conjunction.

The procedure to find the best fit of the model to the data consists in minimizing the χ^2 of the residuals between model and data. This is not an easy task in view of the numerous adjustable parameters. Applying standard methods such as the SIMPLEX algorithm (Caceci

¹⁰This is not realistic because a dwarf nova in quiescence is not expected to have a steady state accretion disk. However, in view of all the other approximations made here this assumption should be sufficient for a rough estimate of the isophotal wavelength of the light curve data; the more so considering the small dependence of the model fits on λ_{iso} .

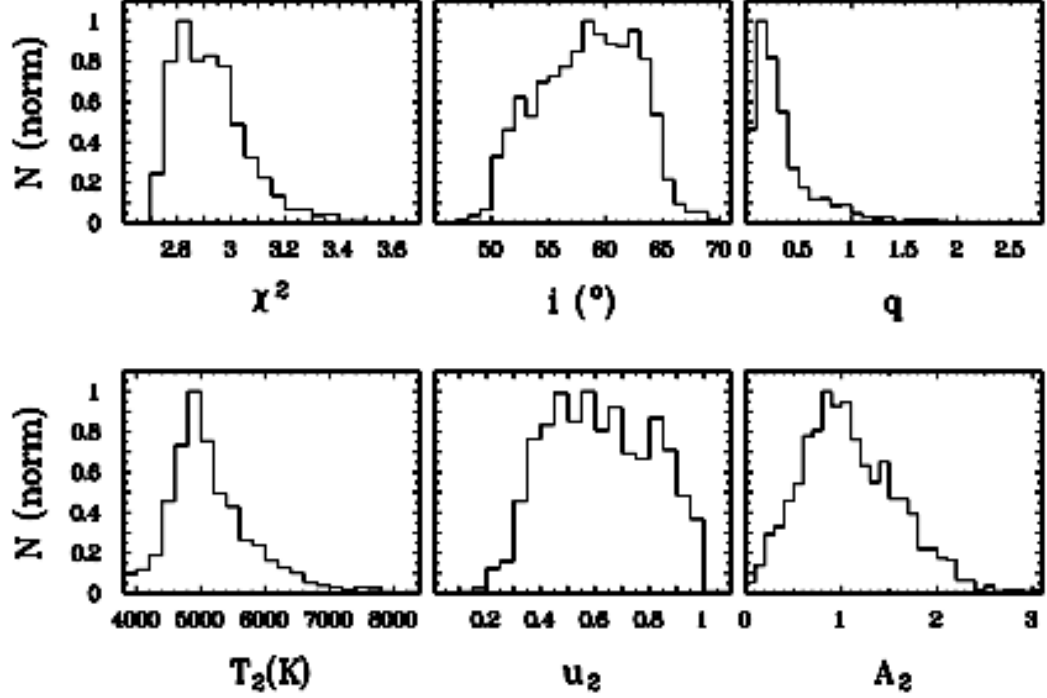


Figure 10: Normalized distribution of χ^2 and of the best fit values for the most relevant system parameters (orbital inclination i , mass ratio $q = M_2/M_1$, secondary star temperature T_2 , limb darkening coefficient of secondary u_2 , and secondary star albedo A_2), constructed from the results of numerous model fits. See text for details.

& Cacheris, 1984) it is quite likely to get stuck in a local minimum of the multidimensional χ^2 surface instead of finding the global minimum. Therefore, a statistical approach is preferred here.

To this end, 1225 trial calculations were performed. In each case initial values for the variable parameters were selected at random within an ample range of plausible choices. These were used to derive a start value for χ^2 . Then each parameter was changed slightly, keeping all others constant, and χ^2 was calculated again. If this yielded a χ^2 smaller than the start value, the parameter set was adjusted to that which resulted in the smallest χ^2 and the entire process was repeated until no further improvement was possible. In this way a parameter set was found which corresponds to the local minimum of the χ^2 -surface nearest to the χ^2 derived using the initial parameters.

The distribution of the minimal χ^2 and of the most relevant system parameters derived from the 1225 trials is shown in Fig. 10. The parameter set corresponding the smallest χ^2 encountered in this exercise was used to calculate the model light curve shown as a solid line superposed upon the observational data in the upper frame of Fig. 9. The difference between data and model results, i.e., the $O - C$ curve, is plotted in the lower frame of the figure. While the overall model fit to the data appears satisfactory, the residuals are not completely random, indicating that the model does not describe the observations perfectly as may be expected in view of the simple parameterization of the primary component which cannot reflect its true structure. Indeed, R statistics (Bruch, 1999) reveal a probability of 98% that the $O - C$ curve contains correlated variations.

In order to obtain a feeling for the goodness of the fit a bootstrap analysis was performed. To this end, a smoothed version of the $O - C$ curve was first generated (broken line in the lower frame of Fig. 9). The probability of correlated variations in the difference between the smoothed and the original $O - C$ curve (which may be termed “second order $O - C$ curve”) is significantly reduced to 57%. The smoothed $O - C$ curve is added to the best fit model light curve which is thus corrected for systematic errors of the model. This light curve is then subjected to random noise with a Gaussian distribution and a variance equal to the variance of the second order $O - C$ curve, generating thus a simulated observational light curve. Finally, the χ^2 between this curve and the best fit model light curve is calculated. This procedure was repeated 1 000 times. The distribution of the individual χ^2 values then yields a statistical error $\sigma_{\chi^2} = 0.40$.

The total range of the χ^2 distribution shown in the upper left frame of Fig. 10 is 0.82. This is only $2.05\sigma_{\chi^2}$. The global minimum of the χ^2 hypersurface is therefore not expected to be much deeper than any of the local minima found in the trial calculations because otherwise a larger dispersion of the individual χ^2 values should be observed. Thus, all of the trial fits which led to this distribution are statistically acceptable. Consequently, the same is true for the model parameters shown in the figure, although in this case physical considerations may constrain some of them.

One of these cases is the albedo \mathcal{A}_2 of the secondary star. The distribution peaks close to $\mathcal{A}_2 = 1$ (lower right frame of Fig. 10; the median values is $\mathcal{A}_2 = 1.0$), but has a long tail to values >1 . Since re-distribution of radiation incident upon the secondary star from outside the rather broad observed wavelength range at a scale leading to an apparent albedo of up to 3 is quite unlikely, values of \mathcal{A}_2 significantly larger than 1 may be considered unphysical. Nevertheless, the model results indicate that the albedo of the MU Cen secondary is high. Rafert & Twigg (1980) have shown that on average $\mathcal{A} \approx 1$ and $\mathcal{A} \approx 0.5$ for stars with radiative and convective envelopes, respectively. The assumed temperature of the MU Cen secondary should place it into the latter category, contrary to what is found here. However, the albedo of individual stars can deviate strongly from the average. At least in one case (RX Ari; a detached binary star) Rafert & Twigg (1980) find $\mathcal{A} \approx 1$ for a star with a considerably lower temperature than the MU Cen secondary¹¹.

For the limb darkening of the secondary star anything more sophisticated than a simple linear law of the kind $I(\mu)/I(1) = 1 - u(1 - \mu)$ is not justified in view of the uncertainties inherent in the present approach. Here, $I(1)$ is the specific intensity at the centre of the stellar disk, and $\mu = \cos \gamma$, where γ is the angle between the line of sight and the emergent radiation. The distribution of u_2 (Fig. 10) is rather broad, with a median value of $u_2 = 0.61$. This is consistent with limb darkening coefficients interpolated in the tables of Claret (2004) at the appropriate values for the effective temperature and wavelength. Likewise, a distribution of the gravity darkening coefficient of the MU Cen (not shown) has a median value of 0.57, which is consistent with the values found in the tables of Claret & Bloemen (2011).

The distribution of the best fit values of the temperature T_2 of the secondary star has a strong peak just below 5000 K. The median is 5017 K. This is consistent with the temperatures of the secondaries of other CVs with similar orbital period. Table 2 contains all CVs identified in the most recent on-line version of the Ritter & Kolb catalogue (Ritter & Kolb, 2003) with a period within 0.04 days of that of MU Cen for which relevant data could be found in the literature. Only for two of them direct quotes of the secondary temperature exist (shown in italics in the forth column of the table) but for many more the spectral type has been determined. In order to transform spectral types into temperatures, the average

¹¹Rafert & Twigg (1980) speculate that this result may be artificial due to the possible presence of a hot spot caused by the impact of mass transferred from the second star in the system.

Table 2: Parameters of long period CVs

Name	Period (days)	Spectral tpye (sec.)	Temp. (sec.) (K)	Mass ratio M_2/M_1	Ref.
SY Cna	0.38238	G8	5280	1.18	3
IU Leo	0.37631	K4.5	4490	0.85	13
AT Ara	0.37551	K2	4840	0.79	1
RU Peg	0.3746	K5V	4600	0.88	4,9
CSS0467+49	0.37155	K4.5	4490	0.73	14
QZ Aur	0.35750		5200		2
GY Hya	0.34724	K4-K5	4490		6
CH UMa	0.34318	K5.5	4400	0.43	12
BT Mon	0.33381	G8V	5280	0.84	7
V1309 Ori	0.33261	K6-K8	4130	0.55	5,8
V392 Hya	0.32495	K5-K6	4400	0.55	6
AF Cam	0.32408	K4-M0	4140	0.60	11,13
V363 Aur	0.32124	G7	5280	1.17	10
IPHAS J034511.59+533514.5	0.31390	K5.5	4400	0.83	13
RY Ser	0.3009	K5	4540	0.84	12
AC Cnc	0.30048	K2V	4840	1.02	10

References: (1) Bruch (2003); (2) Campbell & Shafter (1995); (3) Casares et al. (2009); (4) Dunford et al. (2012); (5) Howell et al. (2010); (6) Peters & Thorstensen (2005); (7) Smith et al. (1998); (8) Staude et al. (2001); (9) Stover (1981); (10) Thoroughgood et al. (2004); (11) Thorstensen & Taylor (2001); (12) Thorstensen et al. (2004); (13) Thorstensen et al. (2010); (14) Thorstensen & Skinner (2012)

temperature of luminosity class V stars from Table A1 of Cenarro et al. (2007) was adopted, and the results are given in Table 2. When only a range of types for the CV secondary is quoted in the literature, the temperature corresponding to the centre of this range is chosen. From the scatter of the individual temperatures values at a given spectral type an error of ~ 150 K is estimated. The secondary stars in long period CVs are expected to be slightly evolved. Therefore, the assumption of the temperature of a main sequence star of the same spectral type introduces a systematic error. In order to estimate its order of magnitude, the average temperature difference between luminosity class V and IV stars in the relevant range of spectral types (G7 - M0) was determined to be ~ 340 K from the list of Cenarro et al. (2007). Thus, the temperatures quoted in Table 2 may be slightly on the high side. Table 2 does not contain any indications of a systematic variation of the secondary temperature within the small range of orbital periods sampled. This is not surprising. Using a smaller data sample, Beuermann et al. (1998) have already shown the significant scatter of secondary spectral types at a given period for periods above ~ 5 hours. The average of the temperature values quoted in Table 2 is 4670 ± 400 K. Within the error limits this is equal to the median of the temperature distribution found for MU Cen.

Disregarding the faint outer wings of the distribution, the best fit values for the orbital inclination i range between 50° and 65° and are somewhat skewed to the upper half of this range. The median value is 58.6° . This is compatible with the absence of eclipses in MU Cen.

Most surprising is the distribution of the best fit values of the mass ratio $q = M_2/M_1$ (upper right frame of Fig. 10). From the radial velocity amplitude in the infrared region,

combined with measurements of the rotational line broadening, Friend et al. (1990) determine $q = 0.83 \pm 0.16$ for MU Cen. This is quite close to the average (0.80 ± 0.22) of the literature values of q for CVs with an orbital period close to that of MU Cen as quoted in the fifth column of Table 2. In contrast, the distribution shown in the figure strongly peaks at quite small values of q and has a long tail to large values, even reaching values much above $q = 1$. The latter may be considered unphysical, meaning that the secondary is much more massive than the primary which would result in unstable mass transfer. But may q really be much smaller than measured by Friend et al. (1990) and expected for CVs with similar orbital periods?

This is quite unlikely. Fig. 11 shows the projection of the χ^2 hyperspace on the $q - i$ and the $q - T_2$ plane, respectively, with all the other variable parameters fixed to the best fit values. The colour code is such that purple refers to χ^2_{\min} , the smallest value encountered in the plane, and red to $\chi^2 \geq \chi^2_{\min} + 3\sigma_{\chi^2}$. It is obvious that for a wide range of mass ratios model solutions can be found which lead to χ^2 within one standard deviation of the best fit value. These results are not restricted to the projections shown in the figure, but repeat themselves in other projections involving q . This means that the model fits are unable to reliably restrict the mass ratio.

Finally, the model calculations permit to quantify the relative contribution of the secondary star to the total light of MU Cen. The best fit model solution implies that on the average over the orbital period the secondary star is 2.75 times brighter than the primary in the observed wavelength range.

5 Discussion

5.1 The period P_2

The light curve of MU Cen was found to contain consistent modulations on two different periods. Apart from the dominating orbital period P_{orb} which is due to ellipsoidal variations of the secondary star, variability on a second period P_2 , slightly longer than $0.5 \times P_{\text{orb}}$ was detected. There is no obvious simple relation between P_2 and P_{orb} . The total amplitude (discounting the scatter due to flickering) of the P_2 modulation is approximately $0^{\text{m}}.07$, while the total orbital amplitude of $\approx 0^{\text{m}}.20$ is almost three times as high. The nature of the P_2 variations is not immediately obvious.

One may speculate that MU Cen is an intermediate polar. In that case the modulation may be due to the variable aspect of a magnetically confined accretion region on the surface of a white dwarf rotating with P_2 . However, there are no further convincing indications for an intermediate polar nature of MU Cen. One of the telltale signatures of such stars are high excitation emission lines in their spectra. In this respect the literature contains ambiguous information: while Warner (1976) mentions the “possible” presence of He II in the quiescent spectrum, it is definitely absent in the spectrum shown by Zwitter & Munari (1996), also taken during quiescence. The ratio between orbital and spin period ($P_{\text{orb}}/P_{\text{rot}} = 1.91$) would be rather unusual – even if not unprecedented – for intermediate polars. Mukai’s list¹² contains only four confirmed systems with $P_{\text{orb}}/P_{\text{rot}} < 2.5$. Moreover, intermediate polars are generally seen in x-rays. But the VizieR data base¹³ does not contain an x-ray source which might be associated with MU Cen. Thus, the evidence for MU Cen to be an intermediate polar is so meager that this hypothesis can probably be discarded.

¹²<http://asd.gsfc.nasa.gov/Koji.Mukai/iphome/iphome.html>

¹³<http://vizier.u-strasb.fr/index.gml>

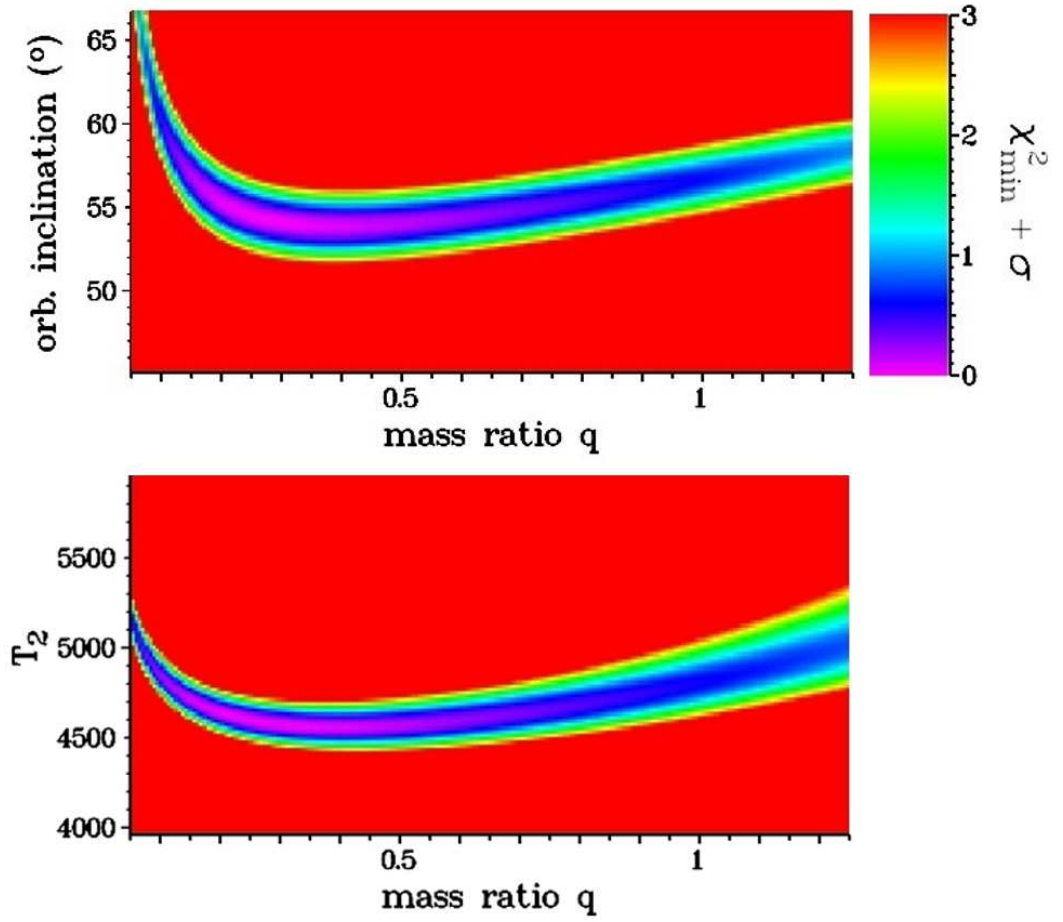


Figure 11: Projection of the χ^2 hyperspace on the $q - i$ and the $q - T_2$ plane, respectively, with all the other variable parameters fixed to the best fit values. The colour code is such that purple refers to χ^2_{\min} , the smallest value encountered in the plane, and red to $\chi^2 \geq \chi^2_{\min} + 3\sigma_{\chi^2}$.

Alternatively, P_2 may be interpreted as the first overtone of a signal with twice that period. The light curve, folded on $2 \times P_2 = 0.3574$ days is shown in the lower right frame of Fig. 4. Not surprisingly, just as in the light curve folded on P_2 , a consistent modulation is apparent; in this case a double humped structure, embraced by a narrow minimum which almost looks like a shallow eclipse. The excess of $2 \times P_2$ over P_{orb} is $\epsilon = (2 \times P_2 - P_{\text{orb}}) / P_{\text{orb}} = 0.045$ which is reminiscent of the period excess typically observed for superhumps. Such features were originally thought to be restricted to superoutbursts of SU UMa type dwarf novae. However, they are increasingly found also in longer period CVs. The on-line version of the Ritter & Kolb (2003) catalogue lists 14 systems with periods above the period gap exhibiting superhumps, although none of them has a period as long as MU Cen¹⁴. Moreover, superhumps are not restricted to accretion disks in their bright state such as dwarf nova in outburst, novalike variables or old novae (Osaki & Kato, 2014). On the other hand, the mass ratio of CVs on average increases with the orbital period. As a consequence of the growth of the superhump period excess with the mass ratio (see, e.g., Smith et al., 2007), ϵ is then also expected to be larger for long period systems. The observed period excess of MU Cen is much smaller than anticipated if the variations were due to a superhump. Furthermore, the shape of the variations (Fig. 4) is quite different from a normal superhump profile.

Thus, I cannot offer a convincing explanation for the origin of the P_2 variations seen in MU Cen and this issue remains open.

5.2 Spectrum vs photometry: a contradiction?

In order for the orbital light curve to be as strongly dominated by ellipsoidal variations as they appear to be one would expect the cool star to leave a strong imprint on the spectrum. However, this seems to be slightly at odds with the available observations. The only published spectrum (Zwitter & Munari, 1996) shows indeed the Na-D lines and possibly other atomic lines in absorption, but neither the line spectrum nor the continuum in the red range exhibit as strong a contribution of a late type star as would be expected in view of the photometric variations.

According to the long term light curves of MU Cen provided by the AFOEV and AAVSO on their respective web-sites, the spectrum of MU Cen was taken at an epoch well separated from the previous and subsequent outbursts. However, on the exact date the AAVSO light curve places MU Cen at a visual magnitude of 14.2. This is 0^m.6 above the mean quiescent V magnitude (Bruch & Engel, 1994) which leaves some margin to reconcile the spectroscopic findings with the present photometric results.

As mentioned in Sect. 4 the secondary star was found to be 2.75 times brighter than the primary component. If the magnitude of MU Cen at the epochs of the present observations was equal to the mean quiescent magnitude of 14^m.78 (Bruch & Engel, 1994), and if the elevated brightness of 14^m.2 at the epoch of the spectroscopic observations of Zwitter & Munari (1996) was due to a brighter primary component, a flux ratio of $F_{\text{sec}}/F_{\text{prim}} = 0.75$ is calculated for that epoch. This may explain why the signature of the secondary star is not as strong in the observed spectrum as might be expected considering its dominance in the light curve.

5.3 Flickering behaviour

One of the initial purposes to observe MU Cen was the verifications of the hitherto not confirmed presence of flickering and the study of its properties. As expected, MU Cen indeed

¹⁴Variations at $P = 0^{\text{d}}.494027$ observed in EY Cyg ($P_{\text{orb}} = 0^{\text{d}}.45932448$) by Costero et al. (2004) are not confirmed as being due to superhumps.

does flicker, however on a comparatively low level compared to most CVs investigated by Beckemper (1995). This can be explained by the strong contribution of the secondary star to the total light. If the secondary star radiation were negligible, as it is in most of the stars of the sample of Beckemper (1995), the flickering amplitude would raise to $0.^m62$, even higher than the average value for quiescent dwarf novae and close to the amplitude observed in strongly flickering systems such as WW Cet and WX Hyi (Beckemper 1995).

The frequency behaviour of the flickering is not unusual when compared to large samples of other CVs. The red noise characteristics, as parameterized by the slope α of the power spectrum on a double logarithmic scale, is within the range observed otherwise, albeit close to its borders. Similarly, the scalegram parameters $\overline{\alpha}$ and Σ , derived from a wavelet analysis of the flickering, place MU Cen within the range occupied by other quiescent dwarf novae. The location close to the lower edge of that range is explained by the dilution of the flickering light source by the strong contribution of the secondary star's light. Night-to-night variations of $\overline{\alpha}$ and Σ are much smaller than observed in most CVs (Fritz & Bruch, 1998).

Interestingly, the stacked power spectra of MU Cen contain indications that flickering events do not occur quite at random but may be correlated, leading to (incoherent) oscillations with slowly evolving amplitudes and frequencies. This may blur the borderline of flickering and what is termed quasi-periodic oscillations in the literature. It may be worthwhile to submit a larger sample of CVs to a systematic study of stacked power spectra of their light curves.

5.4 System parameters

The attempt to pin down system parameters by modelling the light curve was only met with limited success. The inadequacy of the Wilson-Devinney model to describe the primary component of a cataclysmic variable is not considered to be the decisive factor, as long as one refrains from drawing conclusions on the primary's detailed physical properties. I rather attribute the limitations met by the model calculations to the scatter in the phase folded light curve, remaining even after binning as a reflection of the influence of flickering which is not completely cancelled out in the average curve. As a result, many combinations of model parameters lead to calculated light curves which are statistically compatible with the observed one. This inhibits their precise determination.

The model fits permitted to determine only two important system parameters with reasonable certainty. The orbital inclination should lie in the range $50^\circ \leq i \leq 65^\circ$, compatible with the absence of eclipses. A formal Gauss fit to the distribution shown in the lower left frame of Fig. 10 yields 4950 ± 380 K for the temperature of the secondary star, slightly lower than the median value of the distribution cited in Sect. 4. This is in line with secondary star temperatures found in other CVs with similar orbital periods. The less important parameters limb and gravity darkening coefficients are in line with expectations. In contrast, the albedo of the secondary star appears to be higher than expected for a star with a convective envelope. Most unfortunate is the inability to derive an independent estimate for the mass ratio q of MU Cen. Strong correlations with other parameters permit to find parameter combinations which lead to statistically acceptable model fits for a very wide range of q .

Friend et al. (1990) estimated masses of $M_1 = 1.2 \pm 0.2 M_\odot$ and $M_2 = 0.99 \pm 0.03 M_\odot$ for the primary and secondary components, respectively, of MU Cen. Although still within the range observed in CVs in general, M_1 is rather high; significantly higher than the average mass of white dwarfs in CVs which is expected to be of the order of $0.75 M_\odot$ (Knigge, 2006). However, there are two reasons to question the estimated masses.

First, the estimate of Friend et al. (1990) is based on the assumption that the late type

star is on the main sequence. However, it is well known that the secondary stars of CVs are oversized for their mass. Therefore, using their Roche-lobe size together with the main sequence assumption leads to an overestimate of their masses. The present model calculations enabled to delimit the orbital inclination i of MU Cen. Since the radial velocity amplitude of the secondary, together with the orbital period and Kepler’s third law permits to calculate the component masses as a function of i , it is now possible to constrain M_1 and M_2 without taking refuge to the main sequence assumption. For the lower edge of the range of possible inclinations ($i = 50^\circ$), $M_1 = 1.19 \pm 0.22 M_\odot$ and $M_2 = 0.98 \pm 0.26 M_\odot$. Here, the errors were propagated from the errors of the mass ratio and the radial velocity amplitude as quoted by Friend et al. (1990) (the error of the orbital period has only a negligible influence). Adopting the upper edge ($i = 65^\circ$), $M_1 = 0.72 \pm 0.13 M_\odot$ and $M_2 = 0.59 \pm 0.16 M_\odot$. Remembering that the model results indicated a certain preference for higher values of i within the permitted range, the white dwarf mass may thus be close to the average mass found in CVs.

The second effect is harder to quantify. Friend et al. (1990) did not apply a K -correction (see, e.g., Wade & Horne, 1988) to the radial velocity amplitude of the secondary star. This is necessary, if the absorption lines are quenched due to irradiation on the side of the secondary which faces the primary component, resulting in a shift f of the “centre of gravity” of the absorption lines to the opposite side and thus an overestimate of its radial velocity amplitude K_2 . It will also have an effect on the shape of the observed absorption lines and thus on the measured rotational broadening $V_{\text{rot}} \sin i$. Correcting K_2 implies in a smaller orbit and thus, for a given P_{orb} , in smaller component masses. While the K -correction is a linear function of f (Wade & Horne, 1988), the necessary correction for the rotational broadening may well be more complex. Since Friend et al. (1990) used uncorrected values for K_2 and $V_{\text{rot}} \sin i$ to calculate the mass ratio, q will also require a correction which, in turn, has a bearing on the component masses. In order to illustrate the order of magnitude of this effect, and assuming for simplicity that the correction of $V_{\text{rot}} \sin i$ can be neglected, $f = 0.1$ would imply in a larger mass ratio of $q = 0.96$ and a primary star mass lower by 16% in comparison to the uncorrected masses. But, of course, f is not known. In view of the dominant contribution of the secondary star to the total light of MU Cen it is not expected to be large. Therefore, any K -correction will probably have only a small effect on the mass ratio and the component masses.

6 Summary

I have shown that the quiescent light curve of MU Cen is dominated by ellipsoidal variations of the secondary star. This, together with the much longer baseline of the present observations as compared to previously published spectroscopy permitted a more precise determination of the orbital period than was hitherto possible. A second persistent modulation in the light curve with a much smaller amplitude and a period of slightly more than half the orbital period remains enigmatic. Flickering occurs on a rather low level in MU Cen, but only because of the diluting effect of the strong contribution of the secondary star to the total light. The frequency behaviour, as derived from a power spectrum and wavelet analysis, is similar to that found in other quiescent dwarf novae. Flickering events may not always be independent from one another, leading to effects reminiscent of quasi-periodic oscillations. Model fits to the ellipsoidal variations yielded plausible values only for the temperature of the secondary star and for the range of the orbital inclinations compatible with the observations. Other important system parameters, in particular the mass ratio, could not be constrained due to strong parameter correlations. The range of permitted masses for

the primary includes the average mass of white dwarfs in cataclysmic variables. All in all, the only feature which may distinguish MU Cen from a garden variety dwarf nova is the unexplained period P_2 .

References

- Beckemper, S. 1995, Statistische Untersuchungen zur Stärke des Flickering in kataklysmischen Veränderlichen, Diploma thesis, Münster
- Beuermann, K., Baraffe, I., Kolb, U., & Weichold, M. 1998, A&A, 339, 518
- Bruch, A. 1992, A&A, 266, 237
- Bruch, A. 1993, MIRA: A Reference Guide (Astron. Inst. Univ. Münster)
- Bruch, A. 1999, AJ, 117, 3031
- Bruch, A. 2003, A&A, 409, 647
- Bruch, A. 2014, A&A, 566, A101
- Bruch, A., & Engel, A. 1994, A&AS, 104, 79
- Caceci, M.S., & Cacheris, W.P. 1994, Byte, May 1984, 340
- Campbell, R.D., & Shafter, A.W. 1995, ApJ, 440, 336
- Casares, J., Martínez-Pais, I.G., & Rodríguez-Gil, P. 2009, MNRAS, 399, 1534
- Cenarro, A.J., Peletier, R.F., Sánchez-Blázquez, P., et al. 2007 MNRAS, 374, 664
- Chui, C.K. 1992, *An Introduction on Wavelets*, Academic Press, San Diego
- Claret, A. 2004, A&A, 428, 1001
- Claret, A., Bloemen, S. 2011, A&A, 529, A75
- Costero, R., Echevarria, J., Michel R., & Zharikov, S. 2004, BAAS, 36, 1371
- Dunford, A., Watson, C.A., Smith, R.C. 2012, MNRAS, 422, 3444
- Echevarría, J. 1988, ApSS, 130, 103
- Friend, M.T., Martin, J.S., Smith, R.C., & Jones, D.H.P. 1990, MNRAS, 246, 654,
- Fritz, T., & Bruch, A., 1998 A&A, 332, 586
- Horne, J.H., & Baliunas, S.L. 1986, ApJ, 302, 757
- Howell, S.B., Harrison, T.E., Szkody, P., & Silvestri, N.M. 2010, AJ, 139, 1771
- Jawerth, B. & Sweldens, W. 1994, SIAM Rev., 36, 337
- Knigge, C. 2006, MNRAS, 373, 484
- Lomb, N.R. 1976, ApSS, 39, 447
- Mumford, G. 1971, ApJ, 165, 369
- Nohlen, C. 1995, Das Frequenzverhalten des Flickering von kataklysmischen Veränderlichen, Diploma thesis, Münster
- Oskaki, Y., & Kato T. 2014, PASJ 66, 15
- Peters, C.S., & Thorstensen, R. 2005, PASP, 117, 1386
- Rafert, J.B., Twigg, L.W. 1980, MNRAS, 193, 79
- Ritter, H., Kolb, U. 2003, A&A, 404, 301
- Scargle, J.D. 1982, ApJ, 263, 853
- Scargle, J.D., Steiman-Cameron, T.Y., & Young, K. 1993, ApJ, 411, L91
- Schwarzenberg-Czerny, A. 1989, MNRAS, 241, 153
- Schwarzenberg-Czerny, A. 1991, MNRAS, 253, 189

- Smith, A.J., Haswell, C.A., Murray, J.R., Truss, M.R., & Foulkes, S.B. 2007, MNRAS 378, 785
- Smith, D.A., Dhillon, V.S., & Marsh, T.R. 1998, MNRAS, 296, 465
- Staude, A., Schwöpe, A.D., & Schwarz, R. 2001, A&A, 374, 588
- Stover, R.J. 1981, ApJ, 249, 673
- Thoroughgood, T.D., Dhillon, V.S., Watson, C.A., et al. 2004, MNRAS, 353, 1135
- Thorstensen, J.R., Fenton, W.H., & Taylor, C.J. 2004, PASP, 116, 300
- Thorstensen, J.R., Peters, C.S., & Skinner, J.N. 2010, PASP, 122, 1285
- Thorstensen, J.R., Skinner, J.N. 2012, AJ, 144, 81
- Thorstensen, J.F., & Taylor, C.J. 2001, MNRAS, 326, 1235
- Vogt, N. 1976; in: Structure and Evolution of close binary systems, Proc. IAU Symp. 73 (eds.: P. Eggleton et al.); Reidel, Dordrecht; p. 147)
- Vogt, N. 1981, SU UMa - Sterne und andere Zwergnovae, Habilitationsschrift, Universität Bochum
- Vogt, N. 1983, A&AS 53, 21
- Wade, R.A., & Horne K. 1988, ApJ, 324, 411
- Warner, B. 1976, in: Structure and Evolution of close binary systems, Proc. IAU Symp. 73 (eds.: P. Eggleton et al.); Reidel, Dordrecht, p. 85)
- Warner, B. 2004, PASP, 116, 115
- Wilson, R.E. 1979, ApJ, 234, 1054
- Wilson, R.E., Devinney, E.J. 1971, ApJ, 166, 605
- Zacharias, N., Finch, C.T., Girard, T.M., et al. 2013, AJ, 145, 44
- Zwitter, T., & Munari, U. 1996, A&AS, 117, 449